Eur. Phys. J. B **5**, 251–255 (1998)

THE EUROPEAN PHYSICAL JOURNAL B

Highly anisotropic elasticity of a dendrimeric liquid crystal

A.J. Jin[1,a], M.R. Fisch[1,b], M.P. Mahajan[1], K.A. Crandall[1,c], P. Chu[2], C.-Y. Huang[1], V. Percec[2], R.G. Petschek[1], and C. Rosenblatt[1,2,d]

[1] Department of Physics, Case Western Reserve University, Cleveland, Ohio 44106, USA
[2] Macromolecular Science, Case Western Reserve University, Cleveland, Ohio 44106, USA

Received: 23 February 1998 / Revised and Accepted: 26 May 1998

Abstract. Magnetic and electrical Freedericksz measurements were performed on the second generation monodendritic liquid crystal G_2(OH). The deduced elastic constants were found to be exceptionally anisotropic: the splay elastic constant K_{11} is more than an order of magnitude larger than the bend elastic constant K_{33}, and the twist constant K_{22} is approximately twice K_{33}. The results are discussed in terms of molecular conformations.

PACS. 61.30.Gd Orientational order of liquid crystals; electric and magnetic field effects on order

1 Introduction

Dendrimers and hyperbranched polymers are macromolecular compounds which contain a branching point in each structural repeat unit [1–5]. The shape of the three-dimensional architecture resulting from these novel polymers can range from ellipsoidal to cylindrical and spherical. This complex structural capability presents numerous possibilities for new material properties. For example, hyperbranched polymers exhibiting thermotropic calamitic [6], columnar hexagonal [7,8], cubic [9,10], and lyotropic [11] liquid crystalline phases have been reported. Recently we reported the first examples of monodendrons and dendrimers which display thermotropic nematic and smectic phases [12], and examined their pretransitional behavior above the nematic-isotropic phase transition temperature T_{NI} [13]. The purpose of this paper is to report on elastic constant measurements for the monodendron G_2(OH), corresponding to the second generation of the series G_n(OH). Both magnetic and electric Freedericksz transition measurements were performed, whereby an external magnetic (electric) field is applied to an orientationally ordered nematic cell perpendicular to the director $\hat{\mathbf{n}}$. This gives rise to a competition between the elastic restoring force and the magnetic (electric) field, which disrupts the spatially uniform orientation. Above a critical threshold field $\mathbf{H}_{th}(\mathbf{E}_{th})$ — the threshold field is directly related to the elastic constant — the monodomain begins to distort, which may be detectable either optically or electrically. Our central result is that the twist and bend nematic elastic constants differ from typical low molecular weight values and, most significantly, that the bend constant K_{33} is unusually small. The observation that the ratio $K_{11}/K_{33} > 10$, where K_{11} is the splay elastic constant, is very unusual, and indicates that the branched nature or available conformers of G_2(OH) significantly affect the elastic behavior in the nematic phase.

The synthesis of the series of monodendrons G_n(OH) is discussed in references [12] and [14]. A ball-and-stick representation of the molecule G_2(OH) is shown in Figure 1; its detailed chemical composition is shown in Figure 2. The molecular weight of G_2(OH) is $M_n = 3540$. In these structures the 1-triphenyl,1'-alkyl,2-phenyl ethylene spacer in the mesogenic repeat unit is in its *gauche* conformation, as it may exist in isotropic solutions. X-ray diffraction experiments performed in the nematic, smectic, and crystalline phases suggest that in all these phases the mesogenic repeat units are in their *anti* conformation.

In order to determine the elastic constants from the Freedericksz threshold field data, we first obtained both the magnetic susceptibility anisotropy (per unit mass) $\Delta\chi_m[\equiv \chi_{\parallel} - \chi_{\perp}]$ and the dielectric anisotropy $\Delta\varepsilon[\equiv \varepsilon - \varepsilon_{\perp}]$, where $\parallel$ corresponds to values parallel to the director $\hat{\mathbf{n}}$, and $\perp$ to values perpendicular to $\hat{\mathbf{n}}$. $\Delta\chi_m$ *vs.* temperature was obtained with a Faraday susceptometer. The instrument and technique are described in detail elsewhere [15], and the results for $\Delta\chi_m$ are shown in Figure 3. To determine the dielectric anisotropy, a pair of indium-tin-oxide (ITO) coated glass slides was treated

[a] *Present address*: Applied Materials Co., San Jose, CA 95054, USA.
[b] *Permanent address*: Dept. of Physics, John Carroll University, University Hts., Ohio 44118, USA.
[c] *Present address*: Naval Research Laboratory, Washington, D.C. 20375, USA.
[d] e-mail: `cxr@po.cwru.edu`

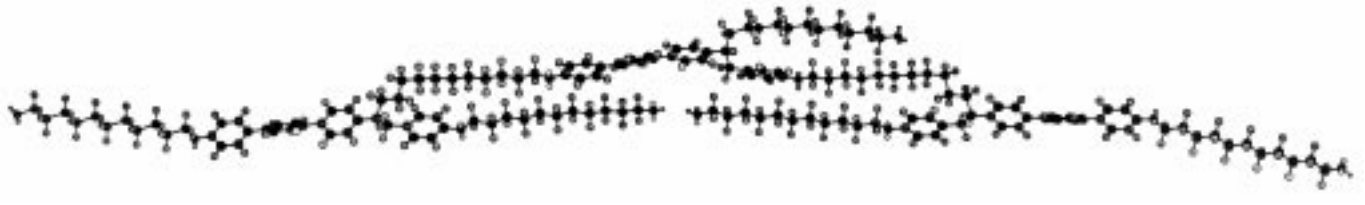

Fig. 1. Ball-and-stick representation of G_2(OH).

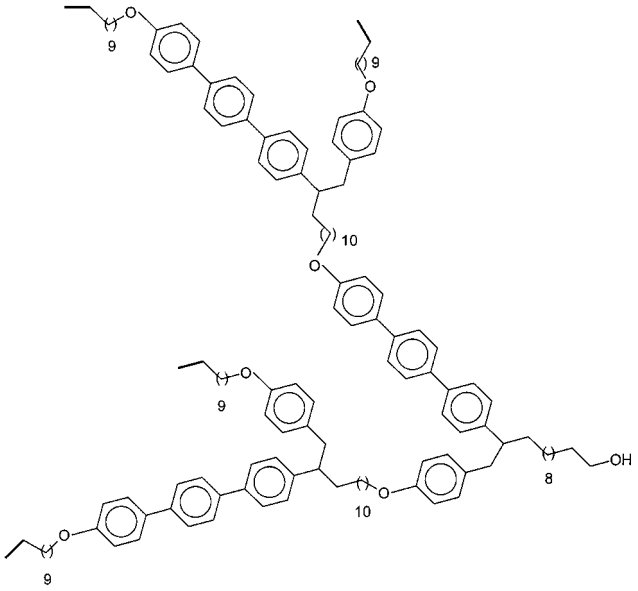

Fig. 2. Chemical structure of G_2(OH).

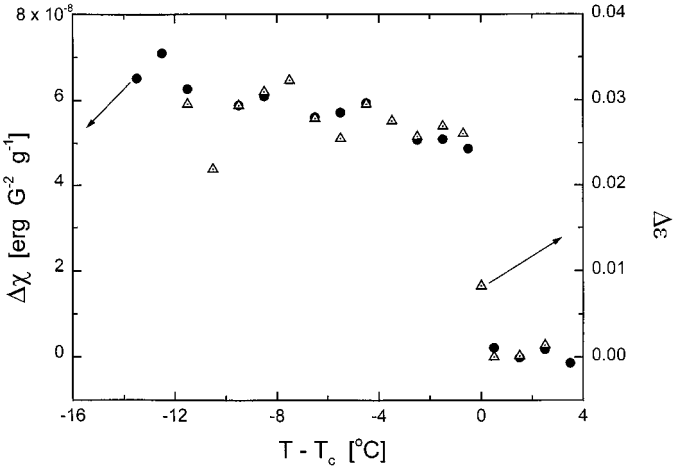

Fig. 3. Measured values of $\Delta\chi_m$(•) and $\Delta\varepsilon$(△) *vs.* temperature.

for homeotropic alignment with the surfactant hexadecyltrimethylammonium bromide (HTAB), separated by mylar spacers of nominal thickness $d = 25\,\mu$m, and cemented together. The current-voltage characteristics of the cell were measured at temperatures above T_{NI} with a lock-in amplifier using a small applied voltage at probe frequency $f_{probe} = 1$ kHz; we thus obtained the isotropic dielectric constant ε_{iso} from an average of these measurements in the isotropic phase. To determine ε we induced uniform homeotropic alignment by applying a large aligning voltage ($\sim$ 75 V rms) well above $\mathbf{E}_{th}$ at frequency $f_{align} = 60$ Hz. We obtained ε from a current-voltage measurement at f_{probe}, and $\Delta\varepsilon \equiv \frac{3}{2}(\varepsilon - \varepsilon_{iso})$ (Fig. 3). This technique is described in detail in reference [16]. For purposes of calculating the elasticities, a smooth curve was drawn through the data.

The bend modulus K_{33} was determined *via* a magnetooptic measurement. Two microscope slides were treated for homeotropic alignment by application of HTAB, then separated by Mylar spacers and cemented together. Using an optical interference scheme [17] the cell spacing d was determined to be $(6.32 \pm 0.05)\,\mu$m. The cell was then filled with liquid crystal and placed into an oven temperature controlled to $\pm 0.1\,^{\circ}$C. The liquid crystal was allowed to align in the nematic phase over four days in a magnetic field of approximately 10 kG. Partially owing to the high viscosity of the dendrimer relative to typical low molecular weight liquid crystals [13], uniform alignment over the several micrometer region required for this experiment was very difficult to achieve; for thicker cells the alignment was unacceptable. The oven-cell assembly was then placed between the poles of an electromagnet, such that was parallel to the cell and perpendicular to $\hat{\mathbf{n}}$. The beam from a 5 mW He-Ne laser passed consecutively through a light chopper, a polarizer oriented at 45° with respect to $\mathbf{H}$, a focusing lens, the cell (with the beam parallel to $\hat{\mathbf{n}}$ for this geometry), an analyzer, and into a photodiode detector. (Note that the cell had to be translated back and forth to locate a well-aligned region through which the beam could pass.) The detector output was fed into a lock-in amplifier referenced to the light chopper, and the output from the lock-in was computer recorded. Owing to the high viscosity of the liquid crystal [13], the magnetic field was very slowly ramped up at a rate of 25 G/s, and the Freedericksz threshold field $\mathbf{H}_{th}$ was determined by a sudden increase in the detector signal. Measurements were performed from approximately 95 °C (the nematic-isotropic phase transition temperature T_{NI}) down to approximately 80 °C. Assuming rigid anchoring conditions, we obtained the bend elastic constant from $K_{33} = \frac{d^2\mathbf{H}_{th}^2\Delta\chi_m}{\pi^2}$ [18];

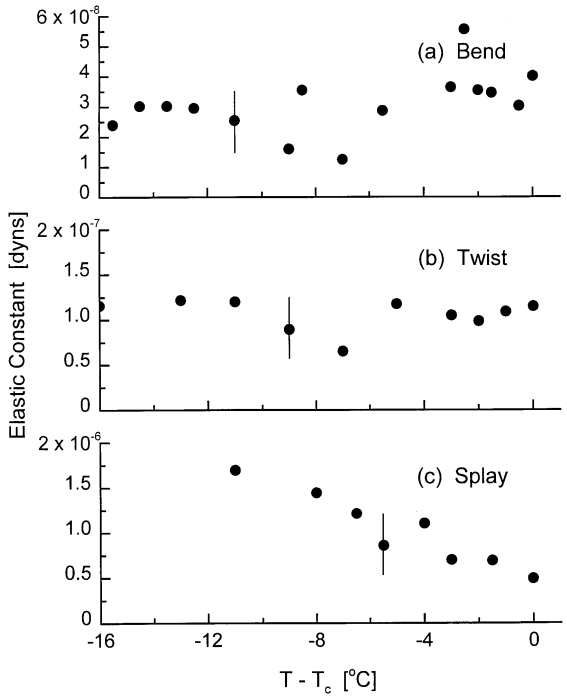

Fig. 4. The three elastic constants *vs.* temperature. Typical error bars are shown.

K_{33} *vs.* temperature is shown in Figure 4a. The relatively large error bars for all the elastic constants are due to the less-than-perfect alignment of the liquid crystal and the very long relaxation times due to the high viscosity. Because we are interested in order(s) of magnitude differences between the various elastic constants, experimental uncertainty of this size is not a major concern.

The twist elastic constant K_{22} was determined similarly. A pair of microscope slides was treated for planar alignment with buffed nylon 6/6, separated by mylar spacers, and cemented together. The thickness was determined to be $d = (6.44 \pm 0.05)$ μm and, after a similar four-day alignment regimen, the oven-cell assembly was placed into the magnet with $\mathbf{H}$ parallel to the cell and perpendicular to $\hat{\mathbf{n}}$. The arrangement of optical components was identical to the arrangement for measuring K_{33}, although in this case the director was perpendicular to the beam direction. For $\mathbf{H} > \mathbf{H}_{th}$ a twist distortion obtained. For thick cells and large optical birefringence the two components of optical polarization would ordinarily follow the director, emerging from the sample with the same orientation and retardation as in the absence of twist distortion. Fortunately the optical birefringence and the thickness are sufficiently small to obviate this situation, resulting in a clear change in the optical signature at $\mathbf{H}_{th}$. Again assuming rigid anchoring conditions, the twist elastic constant is $K_{22} = \dfrac{d^2\mathbf{H}_{th}^2 \Delta\chi_m}{\pi^2}$ [18]; K_{22} *vs.* temperature is shown in Figure 4b.

The splay elastic constant was measured *via* an electrical-field induced Freedericksz technique. This was done for two reasons. First, the inability to obtain uniform alignment over a large area precluded a capacitance determination of $\mathbf{H}_{th}$ in a magnetic field. Second, an optical measurement in a magnetic field, wherein the beam would propagate through the cell parallel to $\mathbf{H}$, would have entailed significant Faraday rotation, thereby obfuscating the desired signal. An electrically-induced/optically-detected Freedericksz transition was therefore chosen. Two ITO-coated slides were coated with nylon 6/6 and buffed unidirectionally. The cells were separated by Mylar spacers and cemented; the thickness was determined to be (6.5 ± 0.2) μm. The geometry of the optical components was identical to that of the twist measurement, except that a Babinet-Soliel compensator was inserted between the crossed polarizers and adjusted to facilitate easy detection of the threshold field. The voltage was stepped up from zero to 80 V over approximately 4 h, and the optical signal was computer recorded. The threshold voltage V_{th} was easily obtained, and the splay elastic constant extracted from the formula $K_{11}\dfrac{V_{th}^2 \Delta\varepsilon}{4\pi^3}$ [18]; K_{11} *vs.* temperature is shown in Figure 4c.

About a decade ago Lonberg and Meyer examined a new striped texture which arises when the splay elasticity is significantly larger than the twist, *via*, $K_{11} > 3.3\,K_{22}$ [19–21]. In that case a twist-splay distortion sets in at a critical field lower than that for a uniform splay distortion in the splay geometry. This result implies that our measured splay elastic constant (Fig. 4c) would, in fact, be a *lower limit* for K_{11}, as the distortion just above $\mathbf{E}_{th}$ would be expected to be a composite twist-splay distortion. Unfortunately unambiguous optical characterization of the nature of the distorted state was not possible. Additionally, based on our very small bend elastic constant (Fig. 4a), one might naively suspect that the measured twist constant is also a lower bound. However detailed calculations [21] demonstrate that in our experimental K_{22} geometry there are no hybrid distortions involving twist, or at least none is second order.

The most striking feature of this data is the very small bend elastic constant. The splay and twist elastic constants are consistent with the usual estimates [18] which are accurate for most small molecules, *i.e.*, the thermal energy divided by the mesogen length. Our measured twist elastic constant is somewhat smaller than the typical estimate, but not extraordinarily so. However the bend elastic constant, which is usually comparable to or larger than the splay elastic constant, is more than an order of magnitude smaller than K_{11}.

It is known that mesogens which are themselves bent may result in decreased bend elastic constants [15,22]. The essential mechanism is that a bent mesogen is better accommodated in a nematic with a macroscopic bend distortion than in an undistorted nematic. Thus macroscopic bend, on average, reorients the mesogens, resulting in both a flexoelectric effect and a decreased bend elastic constant. Similarly twisted mesogens should have a reduction in their twist elastic constants and wedge-shaped mesogens a decrease in their splay elastic constants. This suggests that, to understand the observed elasticities,

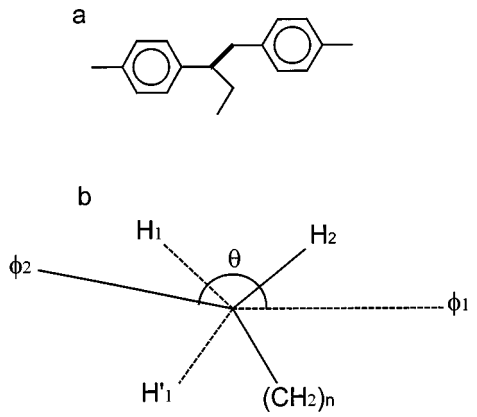

Fig. 5. (a) Structure of mesogen core. (b) Newman diagram for the ethylene spacer (shown by the heavy line in part a) in the mesogen. The symbols are defined in the text.

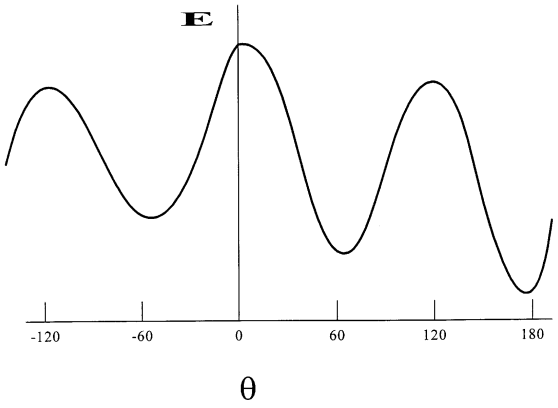

Fig. 6. Energy *vs.* dihedral angle θ between the two phenyls.

we must therefore examine the shape of important configurations of the mesogens. In so doing it is important to remember that many configurations of the mesogen which might be important in free space may not be important in a liquid crystalline phase.

We have previously studied bent dimers [15,22] and found a decrease, albeit relatively small, in K_{33}. These dimers were composed of two rigid segments separated by an odd number of single (sp^3) bonds. Thus the lowest energy configuration – all *trans* (or *anti*) – is *very* bent in the sense that there is a large angle θ between the mesogens. Nevertheless, there are also many nearly unbent dimer configurations, *i.e.*, where θ is small or zero, and these are of comparable energy to the highly bent states. When placed in a nematic field it is likely that the population of highly bent ($\sim 109°$) configurations is strongly suppressed, thereby resulting in the relatively small decrease of K_{33} observed in that system.

The $G_2(OH)$ molecule, on the other hand, is naturally bent, and by an angle sufficiently small to be consistent with a nematic phase. To see this intuitively, one should examine the dihedral angle around the ethylene spacer in the mesogen, shown in Newman projection in Figure 5b. Considering this example as a derivative of a 1,2 diphenyl-alkyl chain, we shall label as ϕ_1 the phenyl attached directly to the carbon; also attached directly to this carbon are two hydrogens, labeled H_1 and H'_1. The other phenyl is labeled ϕ_2, which is attached to a second ethylene-spacer-carbon. Also attached to the second carbon are a hydrogen and alkyl chain labeled H_2 and $(CH_2)_n$, respectively. If the dihedral angle θ is measured between the phenyls, then it might be expected that the lowest lying energy will be that with $\theta = 180°$, *i.e.*, with the bulky phenyls opposite each other – this is the *anti* configuration. There will also be subsidiary minima at $\pm 60°$ – these are the *gauche* configurations. This argument is correct for 1,2 diphenylethylene. However for the actual molecule, while the two phenyls are as distant as possible from each other in the *anti* configuration, this cannot be the lowest energy configuration, as ϕ_1 will be further from the alkyl chain $(CH_2)_n$ by an amount linear in the rotation angle away from 180°. Such a rotation also linearly increases the distance between a hydrogen-hydrogen pair and a phenyl-hydrogen pair, while linearly increasing the distances between two phenyl-hydrogen and one carbon-hydrogen pair. Other distances change only quadratically in the angle change. It is expected that the phenyl-carbon steric interactions will be the most important of these interactions, so that a small decrease in θ will give rise to a net decrease in energy. The resulting energy *vs.* dihedral angle will be similar to that shown in Figure 6.

To confirm this intuition we have performed a restricted Hartree-Fock quantum chemistry calculations with both at the AM1 and 631G* basis sets on the model compound 1,2 diphenyl butane and examined the configurations close to the all *anti* (*trans*) configuration of this molecule. We believe that this configuration is the major contributor in the nematic phase. In the minimum energy configuration we find the angle between the long axes of the phenyls at the restricted Hartree-Fock level with the 631G* basis set is 10°, and the angle between the long axis of the 1-phenyl and the alkyl chain is 35°. This clearly shows that the molecules are bent in equilibrium, and so are expected to have an anomalously low bend elastic constant.

Let us now consider the splay elasticity. The molecule is only somewhat wedge-shaped in the low energy (all *anti*) configurations (Fig. 1), as it has two tails on one side and one tail on the other side. Wedge-shaped molecules are expected to have relatively small splay elastic constants. However the connections between the mesogens are semi-flexible and not rigid. In consequence it is expected that the effect on the splay elastic constant of the wedged-shaped mesogen should be intermediate between that of independent mesogens and that of the lowest energy all *anti* configuration. Other liquid crystal monomers with this approximate "swallow-tail" shape are known [23]. Unfortunately, there are no elastic constant data for this class of molecules, and therefore no reports on the effect of shape (*e.g.*, wedge shaped *vs.* cylindrical) on the elasticity. Detailed theoretical predictions of these effects are difficult, as the packing of aliphatic chains in liquid crystals

is not well understood. Therefore, as the splay elastic constant appears to be similar to that of typical monomer nematics, we believe that the wedge-shape plays little role in determining K_{11} for G_2(OH), perhaps because of molecular flexibility.

We now turn to the twist elasticity. As our G_2(OH) sample is a mixture of chiral enantiomers, it might be expected that it has conformations with large steric twists. However, this does not appear to be the case. In the all *anti* configuration there is no macroscopic twist associated with the chiral center, except for the angle between the plane of the first phenyl in the terphenyl moiety and the plane defined by the phenyl and the alkyl chain. There is substantial torsional freedom along the terphenyl part of the mesogen. The phenyls themselves, particularly in liquid crystalline phases with low symmetry, have interactions that are not too different from those of a disk. Thus we conclude that the monomer does not have appreciable twist and that there is little or no steric or other interaction-based reason for a low twist elastic constant.

Finally, we note that the data show no apparent temperature dependence for the bend and twist elastic constants. We believe that this is an artifact of the difficulty in measuring the elastic moduli, as described above. The not-small error bars are an indication of the this problem. Rather, we have focused our attention in this work on the vast differences in magnitude of the three elastic constants.

In conclusion we have shown that the G_2(OH) dendrimer possesses twist and, in particular, bend elastic constants that are smaller than those of typical low molecular weight liquid crystals. These were examined on the basis of available molecular conformations and resulting average molecular shape.

This work was supported by the National Science Foundation under grant DMR-9122227 and by the NSF's Advanced Liquid Crystalline Optical Materials Science and Technology Center under grant DMR-8920147.

References

1. D.A. Tomalia, Sci. Amer. **5**, 62 (1995).
2. N. Ardoin, D. Astruc, Bull. Soc. Chim. Fr. 875 (1995).
3. J.M.J. Fréchet, Science **263**, 1710 (1994).
4. D.A. Tomalia, H.D. Durst, Top. Curr. Chem. **165**, 193 (1993).
5. F. Vögtle, J. Issberner, R. Moors, Angew. Chem. Int. Ed. Engl. **33**, 2413 (1994).
6. V. Percec, M. Kawasume, Macromol. **25**, 3843 (1992).
7. V. Percec, C.G. Cho, C. Pugh, D. Tomazos, Macromol. **25**, 1164 (1992).
8. V. Percec, G. Johansson, G. Ungar, J. Zhou, J. Am. Chem. Soc. **118**, 9855 (1996).
9. V.S.K. Balagurasamy, G. Ungar, V. Percec, G. Johansson, J. Am. Chem. Soc. **119**, 1539 (1997).
10. S.D. Hudson, H.-T. Jung, V. Percec, W.-D. Cho, G. Johansson, G. Ungar, V.S.K. Balagurasamy, Science **278**, 449 (1997).
11. Y.H. Kim, Am. Chem. Soc. **114**, 4947 (1992).
12. V. Percec, P. Chu, G. Ungar, J. Zhou, J. Am. Chem. Soc. **117**, 11441 (1995).
13. J.-F. Li, K.A. Crandall, P. Chu, V. Percec, R.G. Petschek, C. Rosenblatt, Macromol. **29**, 7813 (1996).
14. V. Percec, P. Chu, Polym. Preprints **36**, 743 (1995).
15. G.A. DiLisi, E.M. Terentjev, A.C. Griffin, C. Rosenblatt, J. Phys. II France **3**, 597 (1993).
16. D. Gu, S.R. Smith, A.M. Jamieson, M. Lee, V. Percec, J. Phys. II France **3**, 937 (1993).
17. C. Rosenblatt, J. Phys. France **45**, 1087 (1984).
18. P.G. DeGennes, J. Prost, *The Physics of Liquid Crystals* (Clarendon, Oxford, 1993).
19. F. Lonberg, R.B. Meyer, Phys. Rev. Lett. **55**, 718 (1985).
20. D.W. Allender, R.M. Hornreich, D.L. Johnson, Phys. Rev. Lett. **59**, 2654 (1987).
21. U. Kini, J. Phys. **47**, 693 (1986).
22. G.A. DiLisi, C. Rosenblatt, A.C. Griffin, J. Phys. II France **2**, 1065 (1992).
23. I. Nishiyama, J.W. Goodby, J. Mater. Chem. **2**, 1015 (1992).